Mixed-solvents MD simlations and hotspots identification

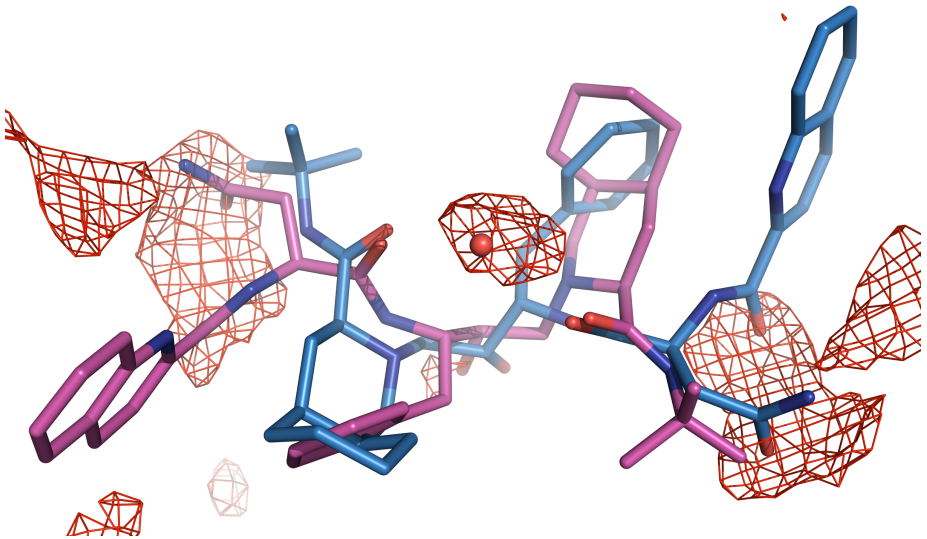

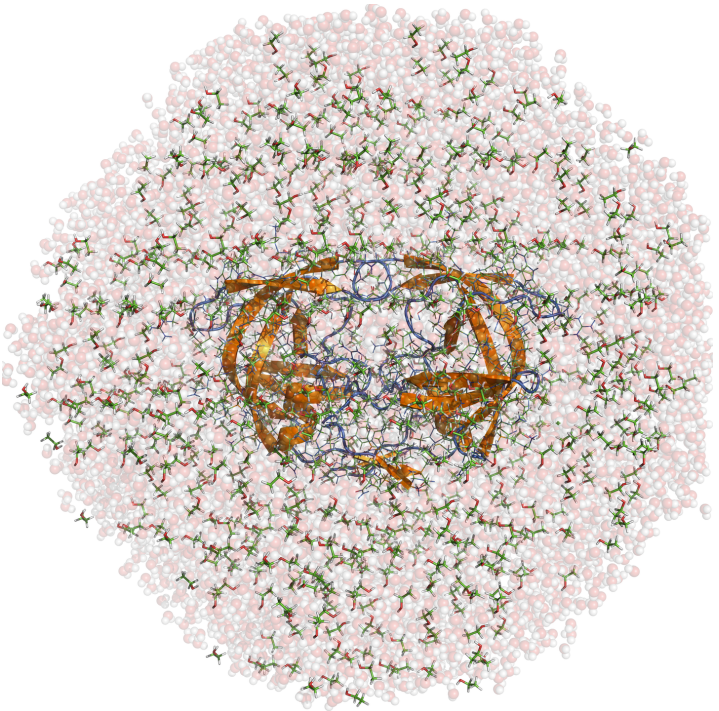

https://sourceforge.net/projects/mdmix/

Motivation and scope

- Importance of identifying binding hotspots in drug discovery
- Limitations of static structural methods (e.g. docking)
- PyMDMix as a mixed solvent MD-based framework tailored for practical hotspot discovery

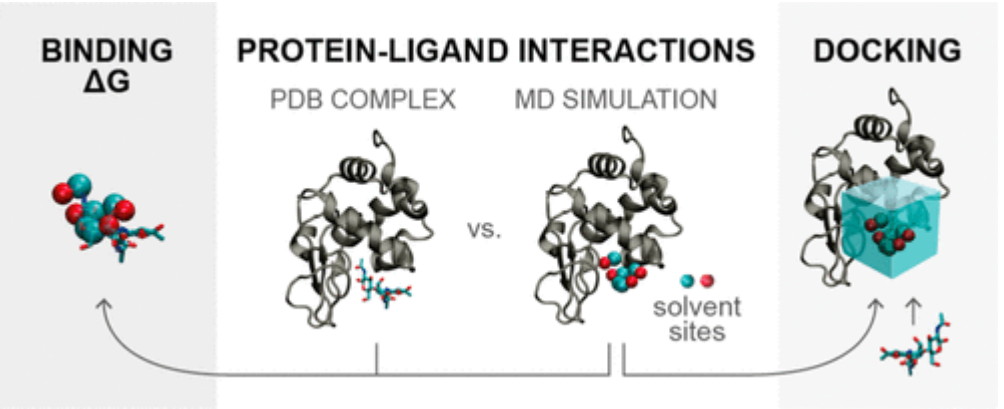

Arcon JP et al. (2017) J. Chem. Inf. Model. 57, 846–863

Historical context

- Origins in Multiple Solvent Crystal Structures (MSCS)
- From rigid mapping (FTMap) to MD-based methods (SILCS, mixed-solvent MD)
- Development of pyMDMix by Barril's group

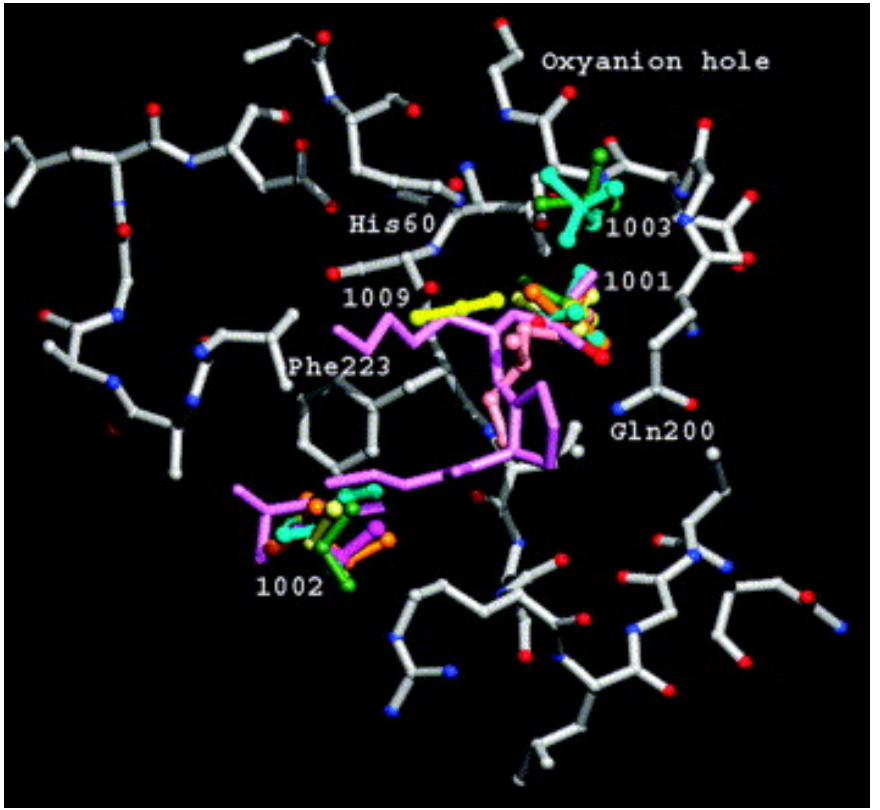

Mattos C et al. (2006) J. Mol. Biol. 357, 1471–1482

Brenke R et al. (2009) Bioinformatics 25, 621–627

Core principles of pyMDMix

- Simulating proteins in water + low-concentration organic probes
- Probes mimic pharmacophoric groups (e.g. hydrophobic, polar, charged)
- Competition with water highlights high-affinity hotspots
- Supports protein flexibility, realistic solvent behaviour

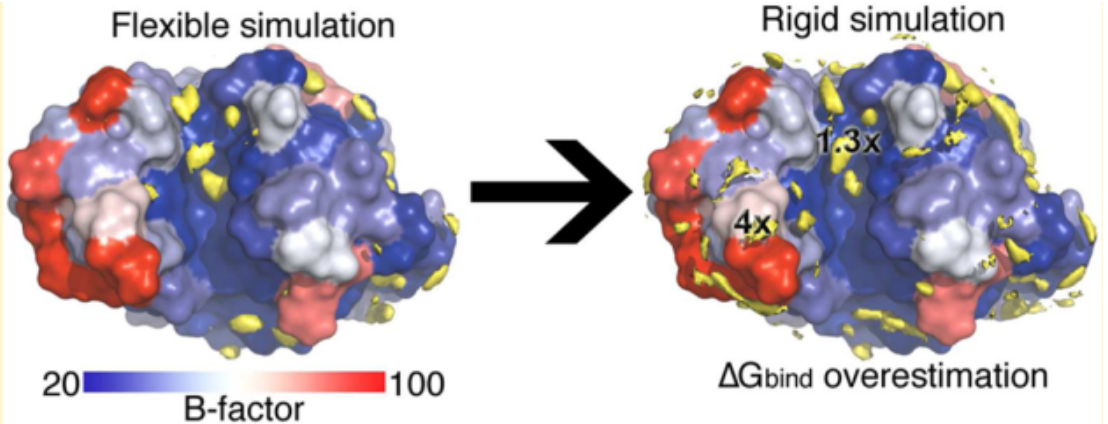

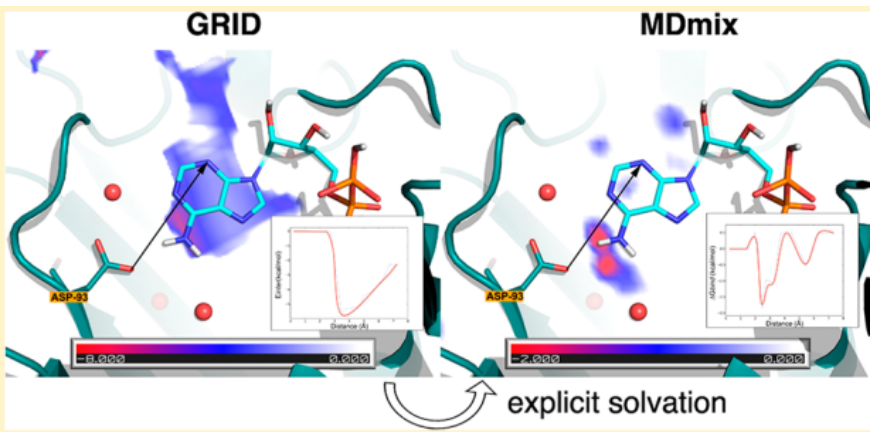

Alvarez-Garcia D et al. (2014) J. Chem. Theory Comput. 10, 2608–2614

Alvarez-Garcia D et al. (2014) J. Med. Chem. 57, 8530–8539

Standard workflow in pyMDMix

- Input: protein structure
- Solvation with water + defined probe types
- AMBER simulations across replicates
- Density map generation
- Energy conversion
- Hotspot identification

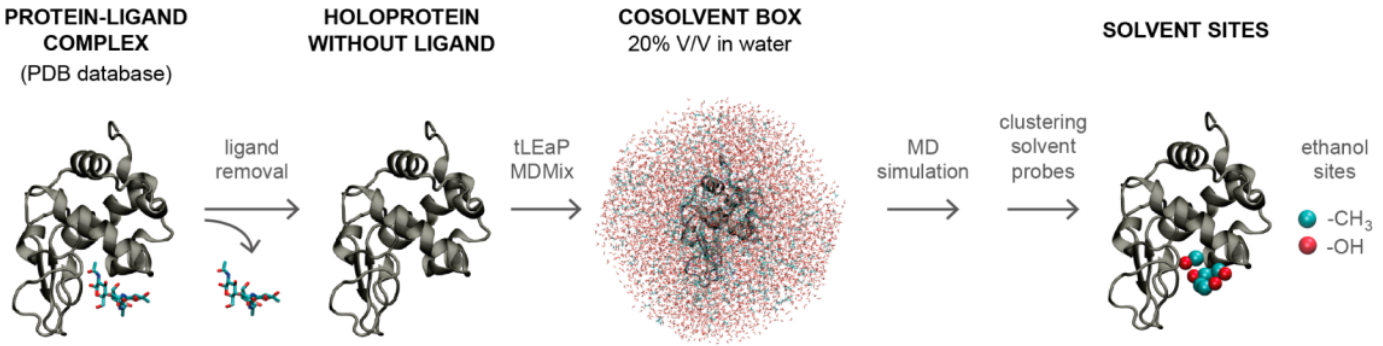

Arcon JP et al. (2017) J. Chem. Inf. Model. 57, 846–863

Analysis and visualization

- 3D probe density maps
- Clustering and interpretation with PyMOL/VMD
- Chemical profiling hotspots (H-bondi hydrophobicity)

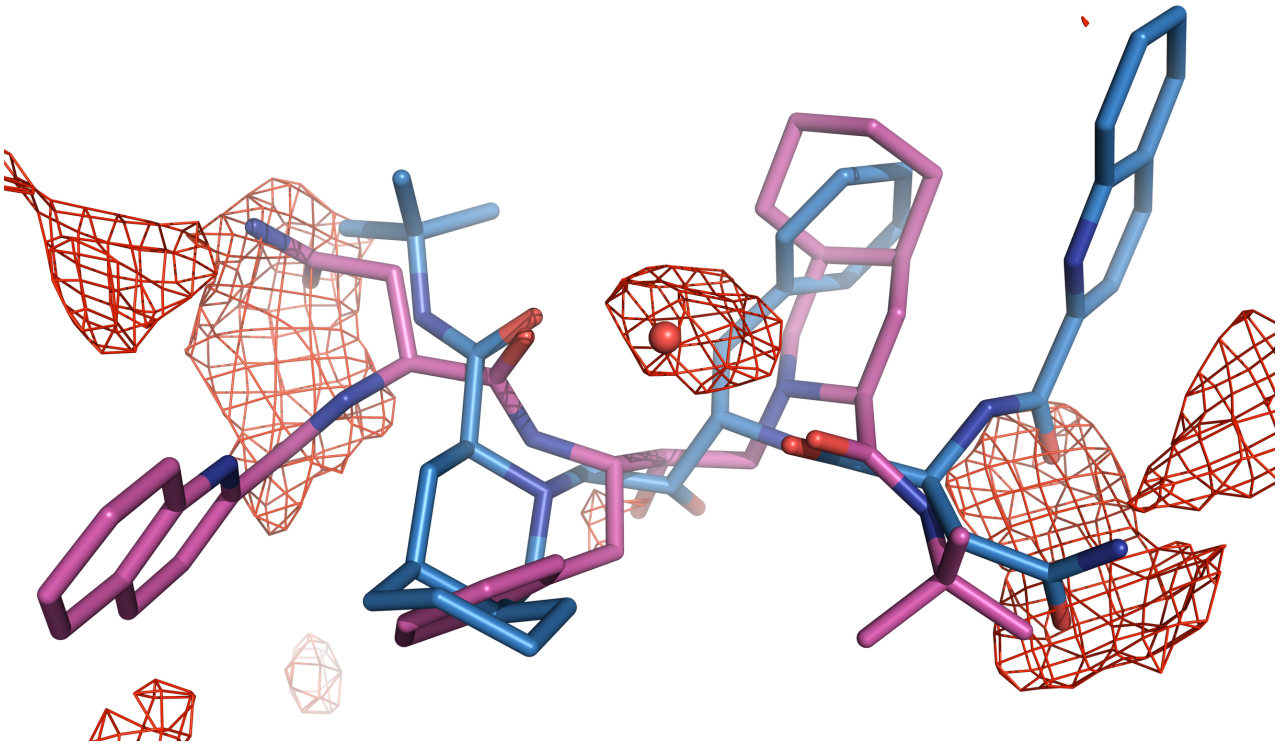

Multi-probe strategy

- Diverse probe types = broader interaction coverage
- Single-probe vs combined probe simulations

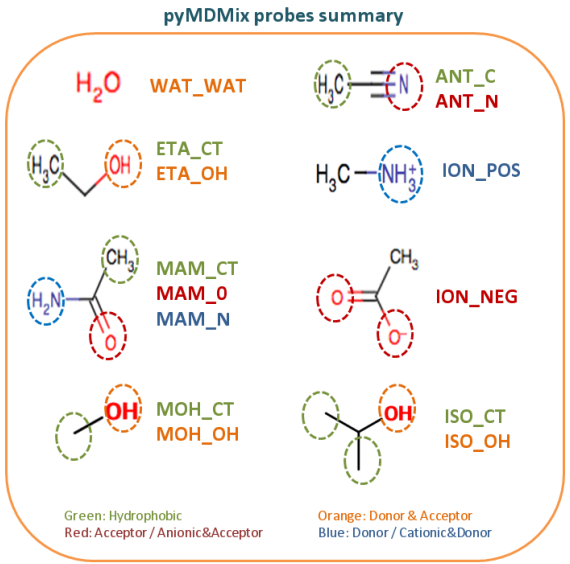

Table 4. Performance of Solvent Probes for the Prediction of Protein–Ligand Interactions

solvent probe	type of solvent site[a]	sensitivity	precision	specificity	accuracy
water	HBD/HBA	0.64 (0.73)	0.33 (0.64)	0.24 (0.43)	0.39 (0.60)
ethanol (−OH)	HBD/HBA	0.36 (0.48)	0.48 (0.63)	0.56 (0.61)	0.45 (0.53)
acetamide ($-NH_2$)	HBD	0.34 (0.39)	0.18 (0.29)	0.62 (0.66)	0.56 (0.59)
acetamide (=O)	HBA	0.27 (0.36)	0.25 (0.38)	0.62 (0.72)	0.51 (0.60)
ethanol ($-CH_3$)	HS	0.72 (0.86)	0.58 (0.96)	0.72 (0.98)	0.72 (0.93)
acetonitrile ($-CH_3$)	HS	0.77 (0.89)	0.54 (0.83)	0.68 (0.88)	0.71 (0.88)
all[b]	HBD/HBA/HS	0.53 (0.64)	0.39 (0.64)	0.56 (0.73)	0.55 (0.69)
all cosolvents[c]	HBD/HBA/HS	0.49 (0.61)	0.42 (0.64)	0.65 (0.77)	0.59 (0.71)

[a]HBD = hydrogen bond donor, HBA = hydrogen bond acceptor, HS = hydrophobic site. [b]"All" includes water, ethanol, acetamide and acetonitrile probes. [c]"All cosolvents" include ethanol, acetamide and acetonitrile probes (it excludes water). Values in parentheses are computed considering only protein–ligand pharmacophoric interaction sites (see text for details).

Arcon JP et al. (2017) J. Chem. Inf. Model. 57, 846–863

Applications – Orthosteric sites

- Recovery of known ligand binding sites
- Confidence in fragment starting points and vector direction

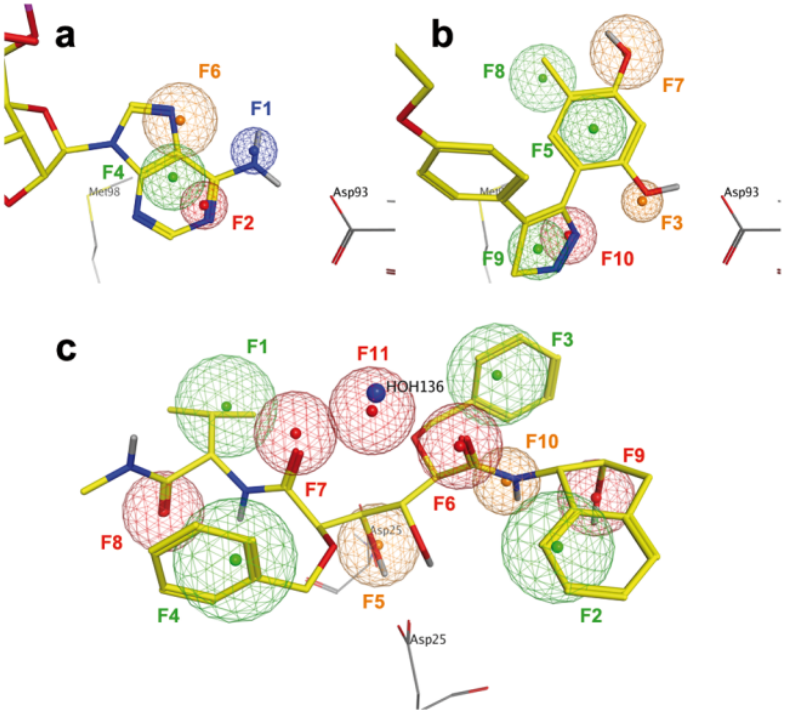

Figure 1. Hsp90 (a,b) and HIVpr (c) pharmacophore models derived from known ligands. For clarity, the pharmacophoric points are shown relative to representative ligands: (a) ADP (PDB code 1BYQ); (b) resorcinol-based inhibitor (2YI6); (c) BEA388, a peptidomimetic inhibitor (1EBZ). Pharmacophore types and radii are shown in Tables 2 and 3.

Schlick T (2010) Springer, New York

Buller A. R. et al. (2013) Proc. Natl. Acad. Sci. U.S.A. 110(8), E653–E661

Applications – Allosteric and cryptic pockets

- Hotspot detection in flexible or hidden regions
- PyMDMix as an alternative to long enhanced MD runs

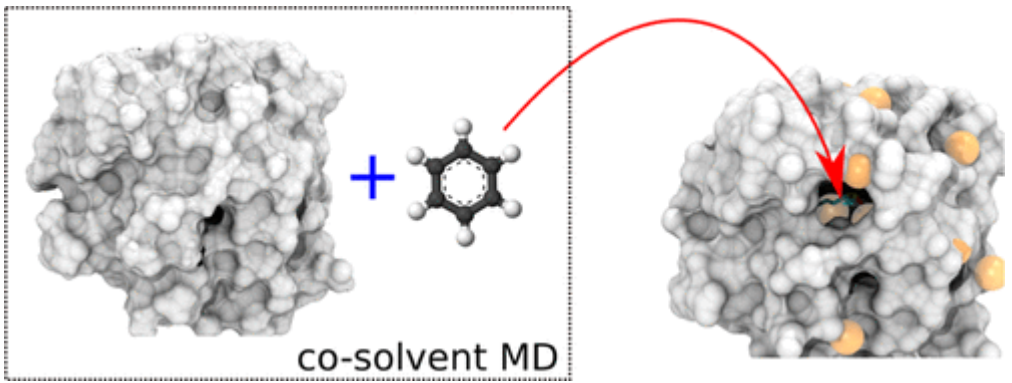

Martinez-Rosell G et al. (2020) J. Chem. Inf. Model. 60, 2314–2324

Fragment-based design

- Probe simulate fragment behavior
- Hotspots guide growth/linking strategies

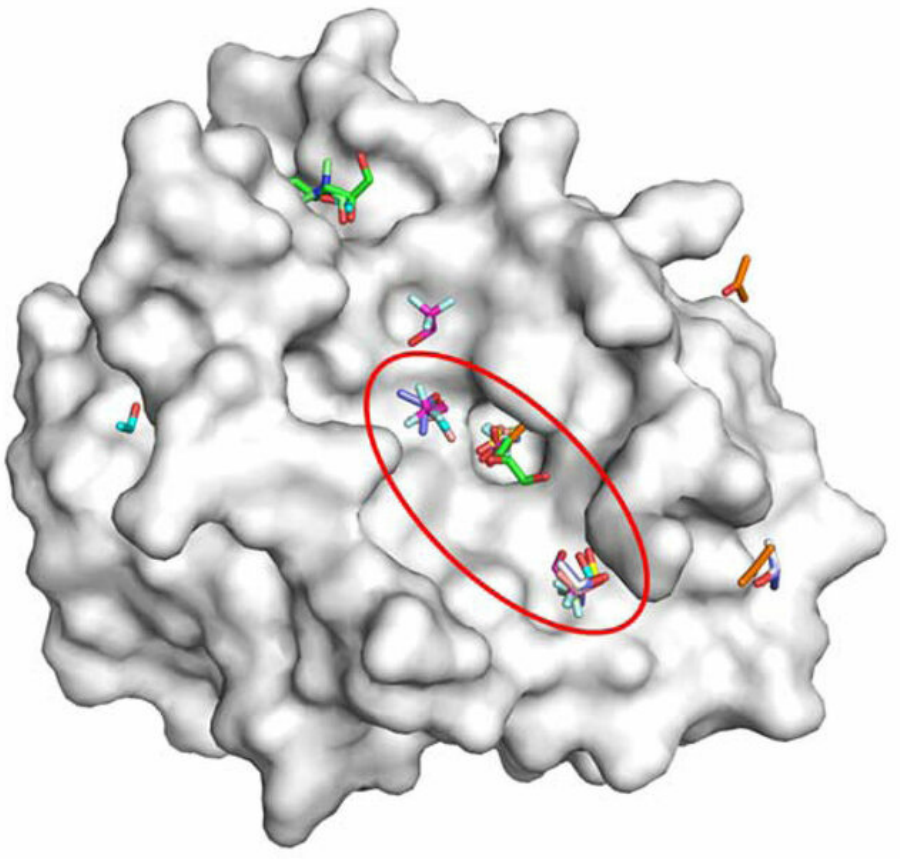

Ghanakota P et al. (2016) J. Med. Chem. 59, 10383–10399

Applications – Water displacement and optimization

- Identifying displaceable structural waters
- Improving binding affinity and selectivity

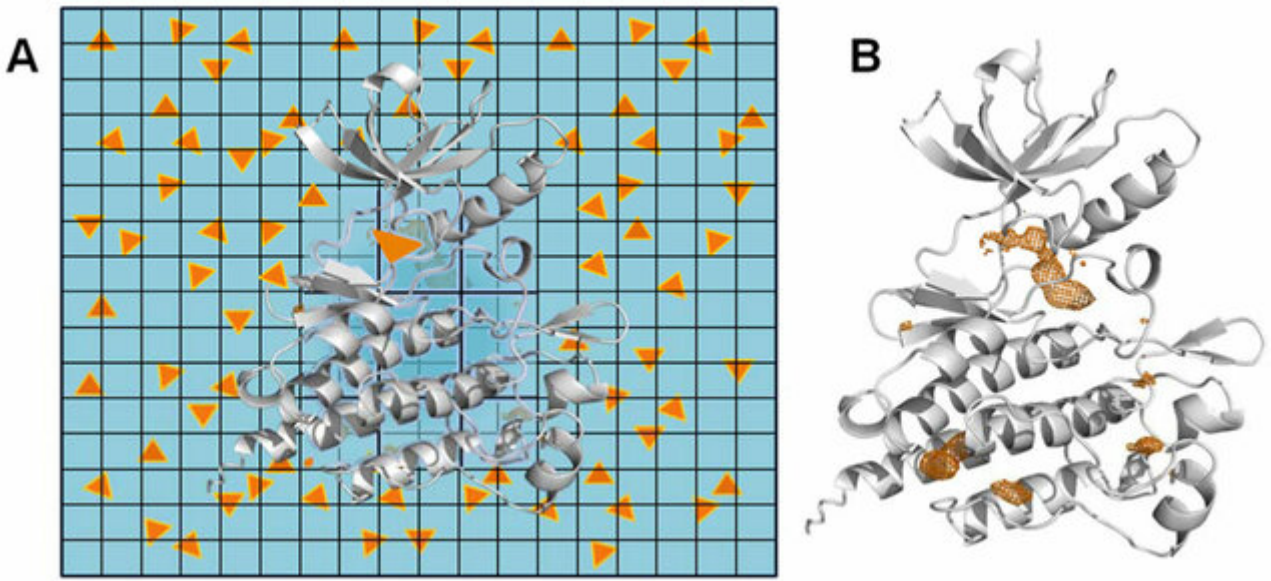

Ghanakota P et al. (2016) J. Med. Chem. 59, 10383–10399

Applications – Integration with virtual screening

- Filtering docked poses using pyMDMix maps
- Prioritizing high-affinity hotspots for scoring

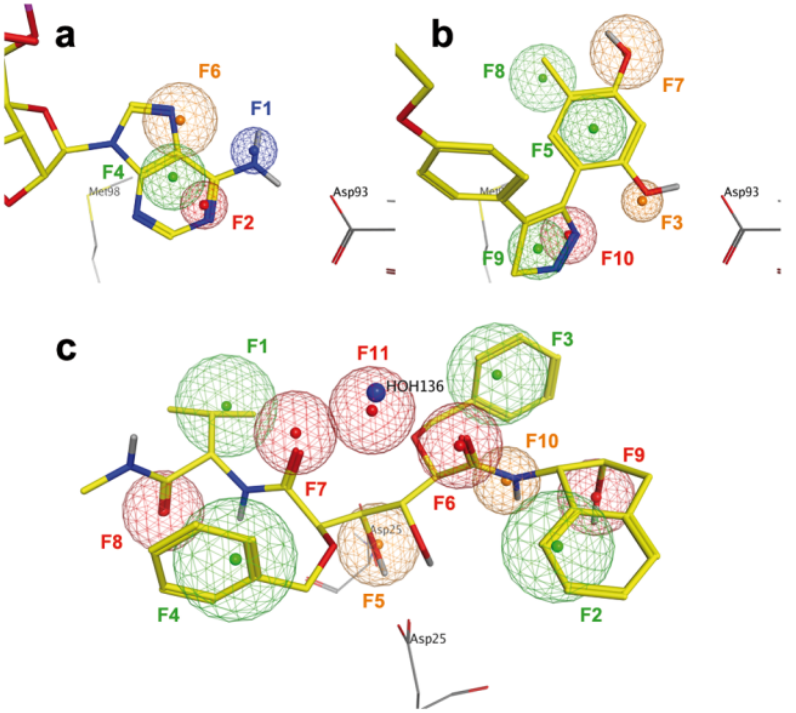

Figure 1. Hsp90 (a,b) and HIVpr (c) pharmacophore models derived from known ligands. For clarity, the pharmacophoric points are shown relative to representative ligands: (a) ADP (PDB code 1BYQ); (b) resorcinol-based inhibitor (2YI6); (c) BEA388, a peptidomimetic inhibitor (1EBZ). Pharmacophore types and radii are shown in Tables 2 and 3.

Cornell WD et al. (1995) J. Am. Chem. Soc. 117, 5179–5197

Lyubartsev A. P. et al. (2016) Biochim. Biophys. Acta Biomembr. 1858(10)

Case study – *Mycobacterium tuberculosis* **PknG**

- pyMDMix recovers acetyl-lysine site
- Validates fragment vectors and expansion paths

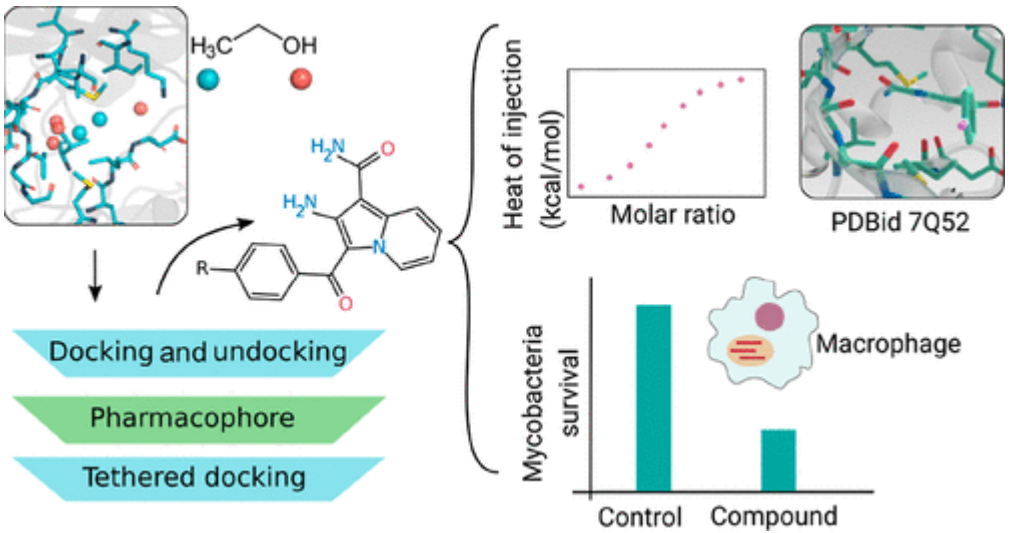

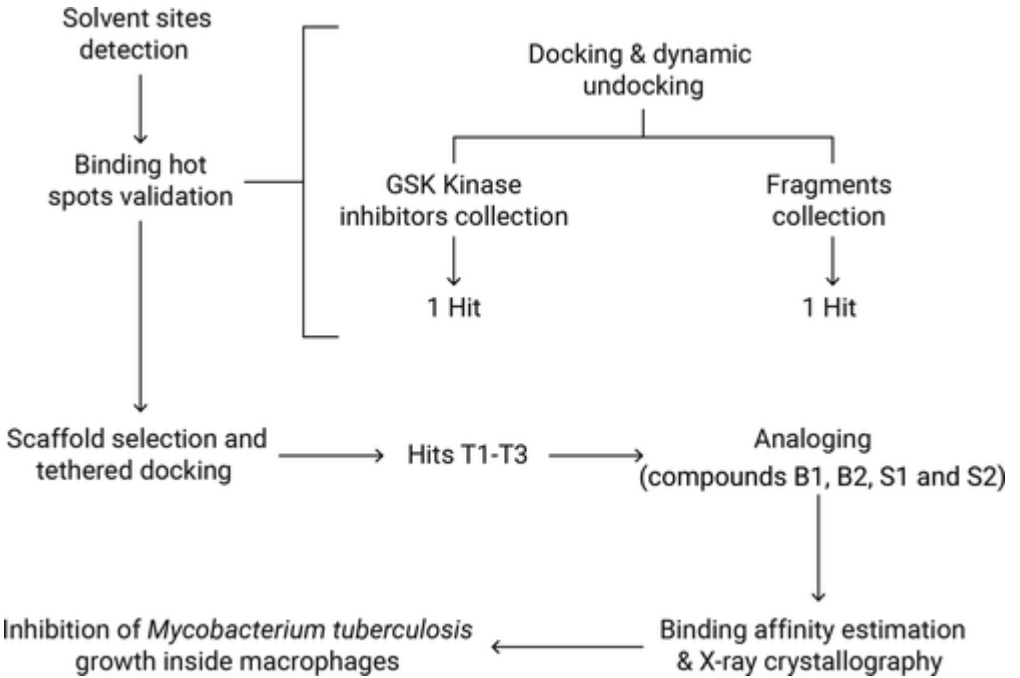

Burastero O et al. (2022) J. Med. Chem. 65, 9691–9705

Case study – ATP synthase (*E. coli*)

- pyMDMix maps used to guide inhibitor design against β subunit
- Virtual screening focused on hotspot clusters
- Identification of micromolar ligands confirmed by bioassays

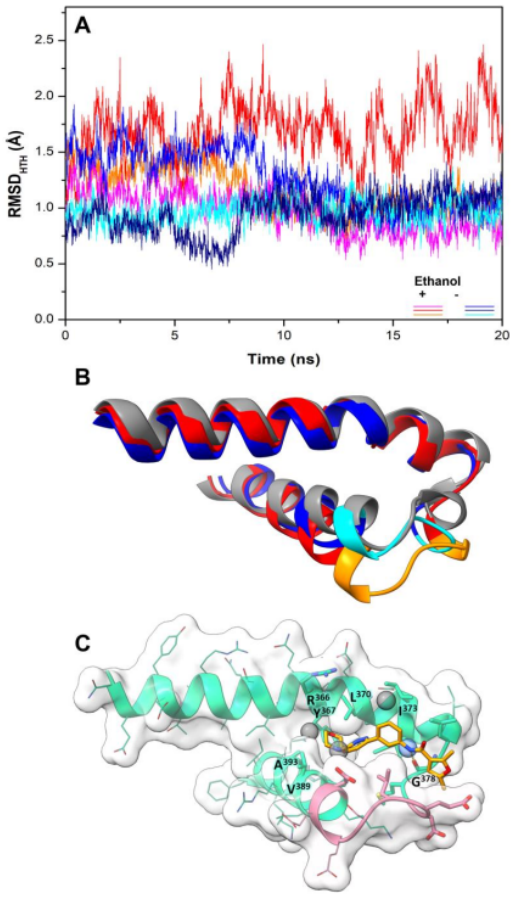

Table 1. Summary of the final active compounds designed against the HTH motif structure of EcF_1.

	Structure [a]	ΔG_{rDock} [b] (kcal/mol)	W_{QB} [c] (kcal/mol)	ΔG_{PB} [d] (kcal/mol)	Residual ATPase Activity (%) [e]	logS [f]
Compd-5	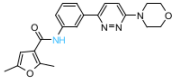	−6.0	8.7	−29	43 ± 6 (50 ± 5%)	−4.7
Compd-7	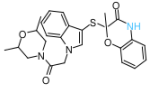	−5.5	6.0	−30	64 ± 12 (70 ± 10%)	−5.1
Compd-14	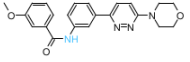	−4.5	6.7	−25	75 ± 8 (73 ± 2%)	−5.3
Compd-15	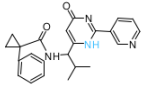	−4.3	6.0	−24	67 ± 5 (ND)	−4.9
Compd-19	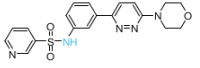	−4.0	6.0	−29	77 ± 7 (70 ± 10%)	−2.8

[a] NH atoms that established hydrogen bonds with the G^{378} backbone oxygen are in blue. [b] rDock score, a weighted sum of intermolecular, ligand intramolecular, site intramolecular and pharmacophoric restraints [44].

Avila-Barrientos LP et al. (2022) Antibiotics 11, 557

Case study – Aurovertin binding site

- pyMDMix reveals allosteric pocket stability and interaction potential
- Free energy decomposition supports druggability of hidden site

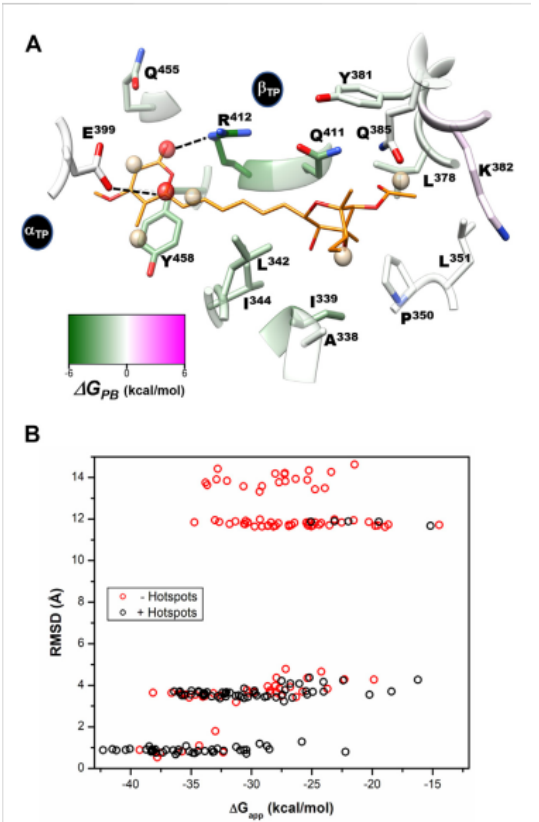

Cofas-Vargas LF et al. (2022) Front. Pharmacol. 13, 1012008

Strengths and limitations

- Strengths: realistic solvation, flexible systems, interpretable data
- Limitations: slow-pocket transitions, sampling bias, probe coverage
- Best used alongside docking, FEP, machine learning

Leach AR. (2001) Molecular Modelling: Principles and Applications.

Rapaport DC. (2004) The Art of Molecular Dynamics Simulation.

Future perspectives

- AI-driven hotspot prediction models trained on pyMDMix outputs
- Automated workflows and integration in discovery pipelines

Leach AR. (2001) Molecular Modelling: Principles and Applications.

Rapaport DC. (2004) The Art of Molecular Dynamics Simulation.

References

- Alvarez-Garcia D, Barril X (2014). J. Med. Chem., 57(19), 8530–8539. https://doi.org/10.1021/jm500320g
- Avila-Barrientos D, et al. (2022). Antibiotics, 11(5), 557. https://doi.org/10.3390/antibiotics11050557
- Cofas-Vargas LF, et al. (2022). Frontiers in Pharmacology, 13:1012008. https://doi.org/10.3389/fphar.2022.1012008
- Burastero O, et al. (2022). J. Med. Chem., 65(14), 9691–9705. https://doi.org/10.1021/acs.jmedchem.2c00499
- Liu Z, Wang P, et al. (2017). J. Med. Chem., 60(11), 4533–4558. https://doi.org/10.1021/acs.jmedchem.6b01800
- Graham SE, Smith RD, Carlson HA (2018). J. Chem. Inf. Model., 58(7), 1331–1342. https://doi.org/10.1021/acs.jcim.8b00154
- Koukos PI, et al. (2021). Brief. Bioinform., 22(4), bbab035. https://doi.org/10.1093/bib/bbab035
- Guterres H, Im W. (2020). J. Chem. Inf. Model., 60(2), 843–862. https://doi.org/10.1021/acs.jcim.9b00951
- Lee J, et al. (2020). Nature Methods, 17, 75–78. https://doi.org/10.1038/s41592-019-0683-1
- Kozakov D, et al. (2015). Nat. Protoc., 10(5), 733–755. https://doi.org/10.1038/nprot.2015.043
- MacKerell AD Jr, et al. (2010). Curr Opin Struct Biol., 20(2), 229–236. https://doi.org/10.1016/j.sbi.2010.01.009
- Schmidtke P, Bidon-Chanal A, Luque FJ, Barril X. (2011). Bioinformatics, 27(9), 1334–1335. https://doi.org/10.1093/bioinformatics/btr127
- Schmidtke P, Barril X. (2010). J. Med. Chem., 53(15), 5858–5867. https://doi.org/10.1021/jm100574m
- Steinkellner G, et al. (2019). Chem. Sci., 10, 5382–5390. https://doi.org/10.1039/C9SC00203F
- Teixeira JM, et al. (2020). Front. Chem., 8:355. https://doi.org/10.3389/fchem.2020.00355
- Humphrey W, Dalke A, Schulten K. (1996). J. Mol. Graphics, 14, 33–38. https://doi.org/10.1016/0263-7855(96)00018-5